

Supporting Information

Photocycle of Photoactive Yellow Protein in Cell-mimetic Environments: Molecular Volume Changes and Kinetics

Cheolhee Yang,^{a,b,†} Seong Ok Kim,^{a,b,†} Yonggwan Kim,^{a,b} So Ri Yun,^{a,b} Jungkweon Choi,^{*,a,b},
and Hyotcherl Ihee^{*,a,b}

- a. Center for Nanomaterials and Chemical Reactions, Institute for Basic Science, Daejeon 305-701, Republic of Korea.
- b. Department of Chemistry, KAIST, Daejeon 305-701, Republic of Korea.

† These authors contributed equally.

*Co-corresponding authors: Jungkweon Choi and Hyotcherl Ihee

E-mail: jkchoi@ibs.re.kr and hyotcherl.ihee@kaist.ac.kr

PYP in the presence of molecular crowding agents with a low molecular weight and size

1. UV-vis and CD spectroscopic measurements

EG and PEGs with various molecular weights are good crowding agents for mimicking the intracellular environment. However, it is known that EG and PEGs with a low molecular weight may induce changes in the structure and stability of a protein due to an attractive interaction for a protein, while Ficoll PM 70, Dextran 40 and BSA have an only pure excluded volume effect for proteins.¹⁻⁵ Therefore, to characterize the structure of PYP in molecularly crowded environments generated by EG and PEGs, UV-vis absorption spectra of PYP in 50 mM Tris-HCl buffer solution (pH 7) were measured as a function of the concentration of molecular crowding agents. Fig. S1 shows the representative absorption spectra obtained as a function of the mass concentration of PEG 400 and PEG 8000, respectively. The UV-vis absorption spectra in the presence of PEG 400 and PEG 8000 are almost identical to that of PYP in the absence of molecular crowding agents. In a similar manner to what was seen for PEG 400 and PEG 8000, the addition of EG does not induce changes in the spectra (not shown). We also measured CD spectra, to investigate whether the secondary structure of PYP changes upon addition of molecular crowding agents. Notably, the CD spectra of PYP above 200 nm are hardly affected by the addition of EG and PEGs, indicating that the α -helix and β -sheet contents of pG are not influenced by the addition of molecular crowding agents (Figs. S1b and S1d). These results suggest that molecular crowding agents, EG and PEGs, do not induce any detectable structural perturbation in PYP.

2. NMR spectroscopic analysis

To further analyze the structure of PYP in the presence of EG and PEGs, we performed NMR experiments using uniformly ¹⁵N-labeled PYP. The chemical shifts of the amide backbone peaks in the ¹H-¹⁵N heteronuclear single-quantum coherence (HSQC) spectrum are well-spread and are identical to those reported in a previous study⁶, that pG adopts the natively folded structure (Fig. S2). Next, we carried out NMR titration experiments using ¹H-¹⁵N HSQC to investigate the interaction between PYP and molecular crowding agents (Figs. S2 and S3). Upon addition of PEG 400, a significant chemical shift perturbation (CSP) was observed in the NH₂ side chain peaks of Gln (Q) and Asn (N) residues, which are polar amino acids located on the exterior surface of PYP (Figs. S3a and S4). To identify the region of PYP that became perturbed upon the addition of PEG 400, the CSP of each residue was calculated in the presence of 20% (v/v) PEG 400 (Fig. S3b), because the peak intensities of PYP in the ¹⁵N-HSQC spectra

decrease dramatically in the presence of a high mass concentration of PEG 400 ($\geq 30\%$ v/v) (Fig. S2). The backbone amide peaks in the N-terminal region (i.e. F6), and polar and acidic amino acids such as Asp (D), Ser (S), and Thr (T) in the flexible loops (i.e. D10, T50 and S72), migrate significantly upon the addition of PEG 400 (Figs. S3b and S3c). Meanwhile, the chemical shifts in structured regions, such as hydrophobic core of the α -helices and β -sheets (i.e. Y76, F92 and M109), are hardly affected by the addition of PEG 400, while the loops between the structured regions are affected (i.e. M100) (Fig. S3c). These observations strongly imply that residues in the N-terminal region and in flexible loops of PYP are preferentially affected by the presence of PEG 400.

The CSP of the critical residues involved in the hydrogen bonding network surrounding the chromophore was further analyzed (Fig. S3c). The peak of C69, which is covalently bonded to *p*CA and is located on a flexible loop, shows only a moderate CSP upon addition of PEG 400. The chemical shifts of Y42 and E46, which play an important role in the photo-activity of PYP through their strong hydrogen bonding network with *p*CA, are not influenced by the addition of PEG 400. The peaks of the amide backbone of T50 and R52, which are polar and located in a loop region, show only a small CSP. Therefore, we conclude that the hydrogen bonding network of the chromophore is well maintained, even in the presence of PEG 400.

A mapping of the perturbed regions of PYP onto the solution structure of PYP (PDB ID: 3PHY)⁷ clearly shows that the most perturbed regions are the exterior flexible loops and the N-terminus. (Figs. S3 and S5). Interestingly, the perturbed residues in the internally structured region are overlap well with the internal water cavity (Fig. S6). This observation suggests that PEG molecules may bind to the flexible N-terminus, to the loops, and near the water cavity in internally structured regions, resulting in dehydration of proteins.

3. SAXS measurements

The effect of PEG on the structure of PYP was also examined by SAXS experiments.⁸ The radius of gyration (R_g) of PYP in the absence of PEG 400 is $15.2 \pm 0.1 \text{ \AA}$, which is consistent with that reported by Imamoto et al.⁹ Fig. S7 shows the R_g values of PYP upon addition of PEG 400 (0–40% v/v). The trend in the R_g values of PYP is similar to that reported by Akabayov et al.¹⁰ Up to 20% (v/v) PEG 400, there is a gradual decrease in the R_g value, indicating compaction of PYP. Considering the results of our NMR experiments, it seems probable that the decrease in the R_g value of PYP in solutions with a low concentration of PEG 400 ($\leq 20\%$ v/v) arises from dehydration, owing to the interaction between PYP and PEG 400. Furthermore,

a molecule of PEG 400 ($R_g = 4.5 \text{ \AA}$)¹¹ has a much larger molecular size than a molecule of water. Therefore, upon addition of PEG 400, the volume available to PYP decreases due to steric exclusion between PEG 400 and the protein, leading to compaction of the protein structure. On the other hand, an increase in the R_g of PYP is observed in solutions containing a high concentration of PEG 400 (>20% v/v). It is established that PEG molecules have compact structures at high concentrations, owing to intramolecular hydrophobic interactions. This compact structure has a smaller excluded volume than the fully extended structure of PEG molecules. Arakawa and Timasheff suggested that the decrease in the excluded volume of PEG 400 leads to an increase in the penetration of PEG molecules into the hydration layer of a protein.¹¹ Consequently, PEG molecules can bind to hydrophobic sites on protein, as well as to the loops, N-terminal helical regions, and near the water cavity in internally structured regions, resulting in increased R_g values. Indeed, several previous studies have suggested the binding of PEG molecules through hydrophobic interactions.¹¹⁻¹³ Such binding may result in an increase of the apparent molecular volume of PYP. Thus, we suggest that the increase in the R_g value of PYP in solutions containing a high concentration of PEG 400 (>20% v/v) probably arises from an increase in the interactions between PYP and PEG 400.

Table S1. Kinetic parameters on the photocycle of PYP determined by TG experiments in the presence of molecular crowding agents

		Kinetic parameters on the photocycle of PYP		
		$\tau_1 / \mu\text{s}$	$\tau_2 / \mu\text{s}$	τ_3 / ms
with EG	0%	$3.3 \pm 1.0^\dagger$	280 ± 13	1.3 ± 0.1
	10%	2.9 ± 0.4	380 ± 9	6.6 ± 0.4
	20%	3.1 ± 0.4	470 ± 7	15 ± 1
with PEG 400	0%	$3.3 \pm 1.0^\dagger$	280 ± 13	1.3 ± 0.1
	20%	3.2 ± 0.5	480 ± 7	12 ± 1
with PEG 1000	0%	$3.3 \pm 1.0^\dagger$	280 ± 13	1.3 ± 0.1
	7%	2.6 ± 0.3	430 ± 8	9.0 ± 2.1
	12%	2.7 ± 0.4	500 ± 12	8.6 ± 1.3
with PEG 8000	0%	$3.3 \pm 1.0^\dagger$	280 ± 13	1.3 ± 0.1
	12%	2.0 ± 0.4	360 ± 10	9.2 ± 0.7
with Ficoll PM 70	0%	$3.3 \pm 1.0^\dagger$	280 ± 19	0.9 ± 0.2
	3%	3.6 ± 0.2	350 ± 14	1.8 ± 0.8
	6%	3.5 ± 0.3	360 ± 13	2.1 ± 2.5
with Dextran 40	0%	$3.3 \pm 1.0^\dagger$	280 ± 8	1.5 ± 0.1
	4%	2.8 ± 0.2	320 ± 7	2.7 ± 0.5
	9%	2.3 ± 0.2	320 ± 9	2.6 ± 2.3

[†] The average value of τ_1 measured in the absence of molecular crowding agents.

Table S2. Kinetic parameters on the photocycle of PYP determined by TA experiments in the presence of molecular crowding agents

		Kinetic parameters on the photocycle of PYP			
		$\tau_1 / \mu\text{s}$	$\tau_2 / \mu\text{s}$	τ_3 / ms	τ_4 / ms
with EG	0%	$4.1 \pm 0.8^\dagger$	340 ± 18	1.8 ± 0.1	120 ± 1
	10%	4.2 ± 1.3	390 ± 20	2.2 ± 0.2	120 ± 1
	20%	4.1 ± 1.2	490 ± 19	3.1 ± 0.3	110 ± 1
with PEG 400	0%	$4.1 \pm 0.8^\dagger$	340 ± 22	1.6 ± 0.1	120 ± 2
	10%	4.0 ± 1.2	430 ± 23	2.2 ± 0.2	150 ± 2
	20%	4.2 ± 1.4	520 ± 24	2.9 ± 0.3	190 ± 3
with PEG 1000	0%	$4.1 \pm 0.8^\dagger$	320 ± 20	1.8 ± 0.1	120 ± 1
	7%	3.9 ± 1.1	430 ± 19	1.8 ± 0.3	160 ± 2
	12%	3.5 ± 0.9	540 ± 17	1.8 ± 0.5	230 ± 3
with PEG 8000	0%	$4.1 \pm 0.8^\dagger$	340 ± 18	1.8 ± 0.1	120 ± 1
	5%	3.2 ± 0.8	380 ± 22	1.9 ± 0.2	130 ± 2
	12%	3.7 ± 1.5	390 ± 24	1.9 ± 0.3	150 ± 2
	23%	3.8 ± 0.1	500 ± 27	1.9 ± 0.3	190 ± 3
with Ficoll PM 70	0%	$4.1 \pm 0.8^\dagger$	280 ± 25	1.2 ± 0.2	120 ± 2
	3%	3.3 ± 1.3	290 ± 22	1.2 ± 0.2	130 ± 2
	6%	2.8 ± 1.9	280 ± 28	1.2 ± 0.2	130 ± 3
with Dextran 40	0%	$4.1 \pm 0.8^\dagger$	290 ± 26	1.3 ± 0.2	120 ± 2
	4%	3.8 ± 2.1	290 ± 24	1.3 ± 0.2	120 ± 2
	9%	3.7 ± 1.7	280 ± 25	1.2 ± 0.2	120 ± 2
with BSA	0%	$4.1 \pm 0.8^\dagger$	330 ± 18	1.8 ± 0.1	120 ± 1
	7% (100 g/L)	3.5 ± 0.9	340 ± 17	1.8 ± 0.1	130 ± 1
	14% (200 g/L)	3.6 ± 1.0	360 ± 16	2.1 ± 0.2	150 ± 2

\dagger The average value of τ_1 measured in the absence of molecular crowding agents.

Fig. S1

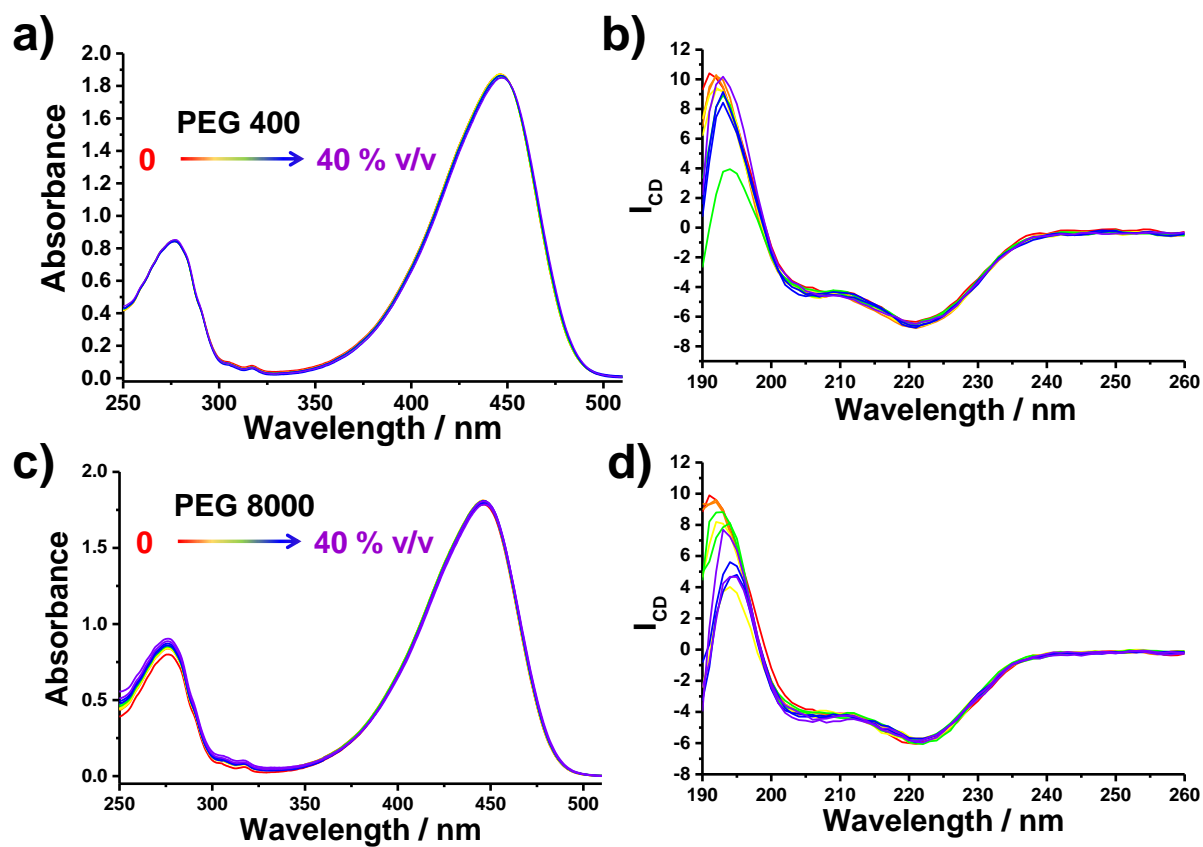


Fig. S1. UV-Vis and CD spectra of PYP and. a and c) UV-Vis absorption spectra of PYP in 50 mM Tris-HCl buffer (pH 7) as a function of the concentration of PEG 400 and PEG 8000, respectively. b and d) CD spectra of PYP in 50 mM Tris-HCl buffer (pH 7) as a function of the concentration of PEG 400 and PEG 8000, respectively.

Fig. S2

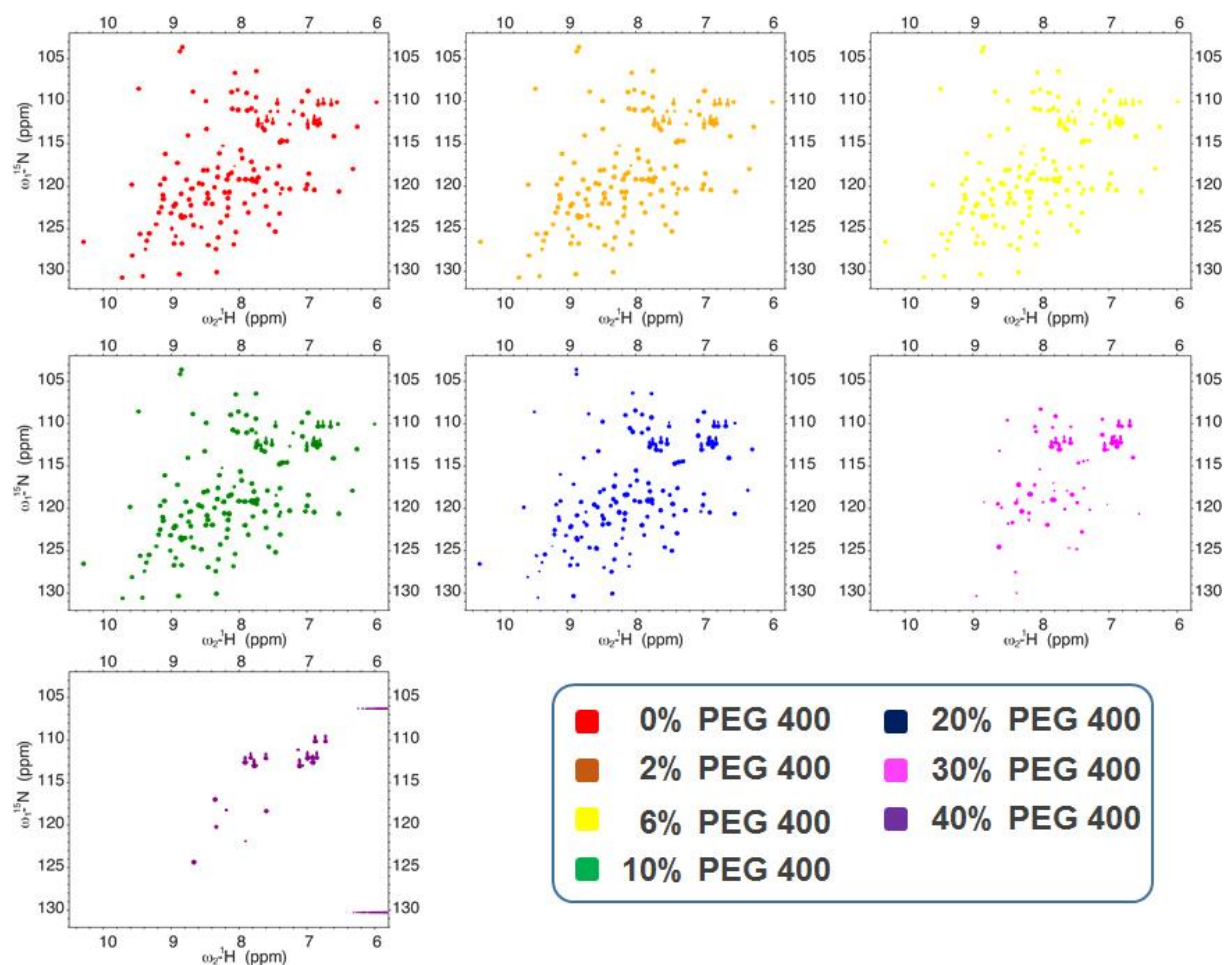


Fig. S2. ^1H - ^{15}N HSQC spectra of PYP in various concentrations of PEG 400. ^1H - ^{15}N HSQC spectra of PYP in 0% v/v PEG 400 as control (red); 2% v/v (Orange); 6% v/v; 10% v/v (Green); 20% v/v (Blue); 30% v/v (Magenta); 40% v/v (Purple). Note that the peak intensity drops dramatically over 30% v/v of PEG 400 addition.

Fig. S3

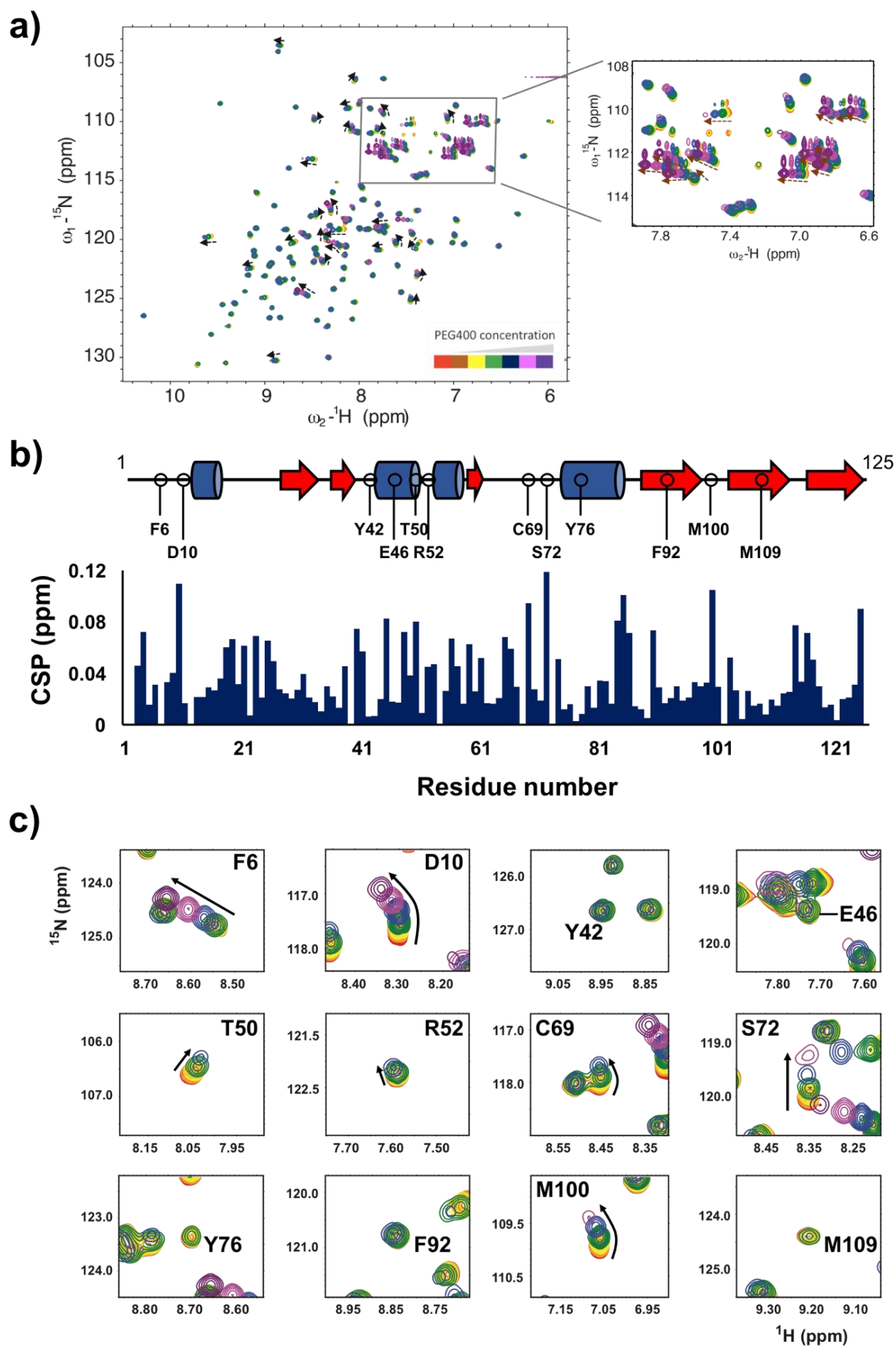


Fig. S3. NMR titration experiments. a) (left panel) Overlaid spectrum of PYP according to the concentration of PEG 400. ^1H - ^{15}N HSQC spectra of PYP in 0 (red), 2 (Orange), 6 (Yellow), 10 (Green), 20 (Blue), 30 (Magenta) and 40% v/v of PEG 400 (Purple). Note that peaks which show strong migration are denoted with black arrows from 0 to 40% v/v of PEG 400 direction. (right panel) Enlarged section of NH_2 side chain peaks of Gln and Asn. Migration of NH_2 side chain peaks of Gln and Asn are denoted with brown arrows from 0% to 40% v/v of PEG 400 direction. Note that peaks of NH_2 side chain of Gln and Asn appear in the upfield of nitrogen dimension with doublet. b) Chemical shift perturbation (CSP) for each residue in the presence of 20% v/v of PEG 400. Secondary structure diagram is aligned with CSP plot for clarity. The α -helixes and β -sheets are designated as dark blue colored cylinders and red colored arrows, respectively. Selected residues in Fig. 2c are designated on the secondary structure diagram in Fig. 2b. c) Overlaid spectra of the selected residues upon an addition of PEG 400. Each residue number and amino acid are labeled in each section. The residues which do not show migration are labeled around the peaks of 0% PEG 400 and the residues which show noticeable migration are labeled in top corner of section with black arrow from 0 to 40% v/v of PEG 400 direction.

Fig. S4

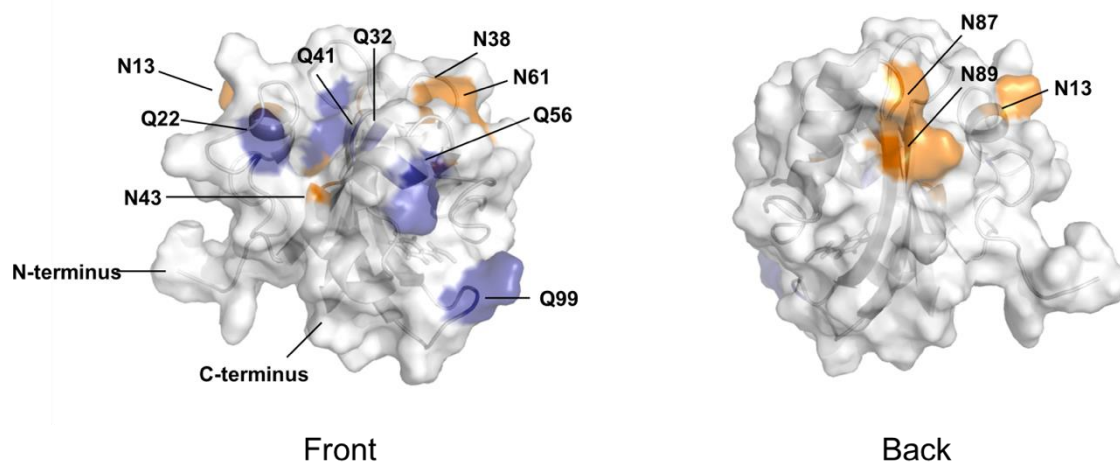


Fig. S4. Position of Asn (N) and Gln (Q) on PYP. Asn (N) and Gln (Q) in the PYP cartoon and surface representation are colored blue and orange, respectively. Most of the Asn and Gln, which are polar amino acid, are located on the exterior surface.

Fig. S5.

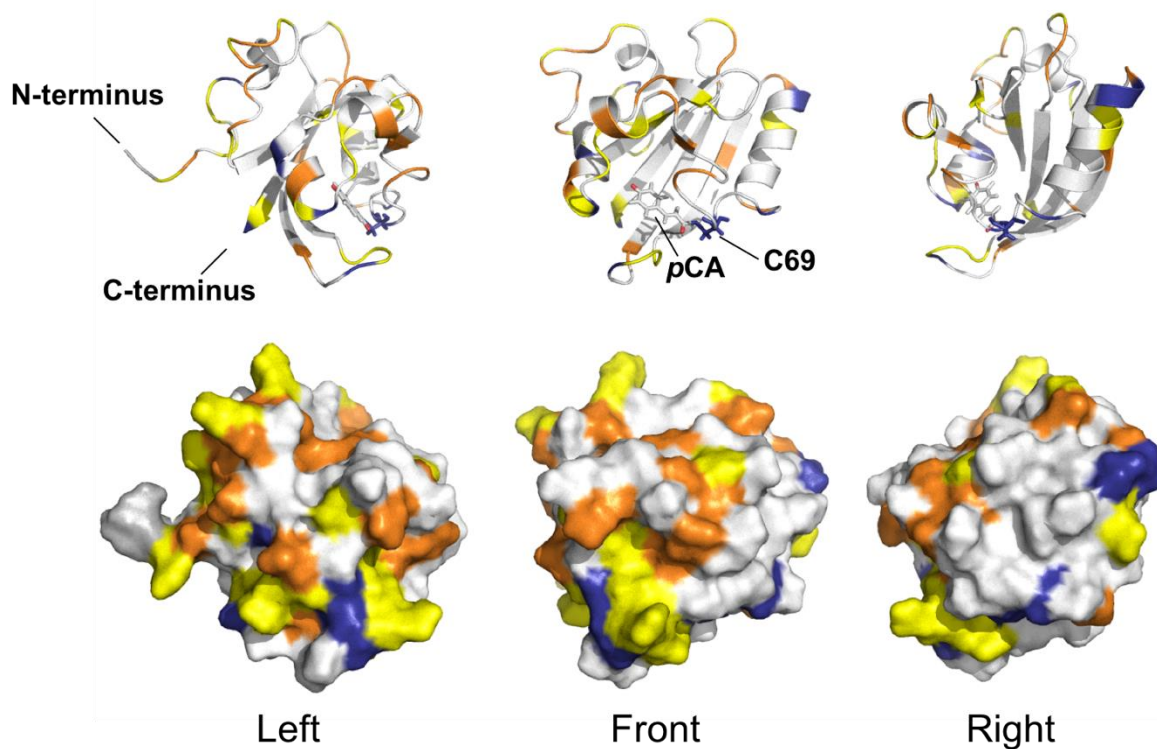


Fig. S5. Mapping of chemical shift perturbation on PYP. (top) Cartoon representation of PYP. (bottom) Surface representation of PYP. CSP colored dark blue, orange and yellow according to the CSP values (>0.08: strong, dark blue colored; 0.05-0.08: moderate, orange colored; 0.03-0.05: weak, yellow colored). Note that peaks in ^{15}N -HSQC spectra of N-terminal 2 residues, denoted as gray color, are disappeared by the addition of PEG 400. Each panel contains three different point views. (left) 60° left point, (middle) front; Cys69 and chromophore, (right) 60° right point view. Most perturbed region is located on a flexible loops and the N-terminus.

Fig. S6

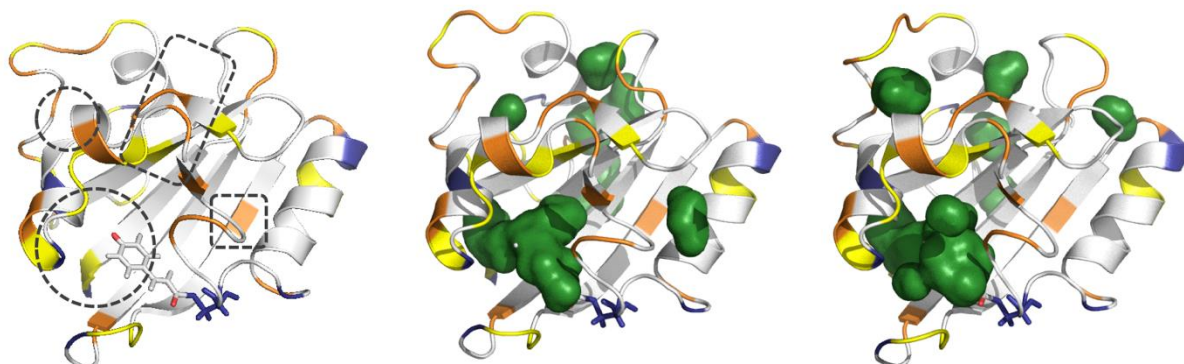


Fig. S6. CSP and water cavity of PYP. (left) Cartoon representation of PYP. (Middle and right) Cartoon representation of PYP with water cavity. Two ensemble structures of PYP are chosen for clarity. Cartoon representation is colored by CSP values and internal water cavity is colored green. The residues are colored according to the corresponding CSP values (>0.08: strong, dark blue colored; 0.05-0.08: moderate, orange colored; 0.03-0.05: weak, yellow colored). Perturbed regions which are not located on the N-terminus, flexible loops and exterior surface is designated by black dotted circle or rectangle in left panel. The internal water cavities are well overlapped with the designated perturbed region. The internal water cavities of PYP are visualized with PyMOL.

Fig. S7

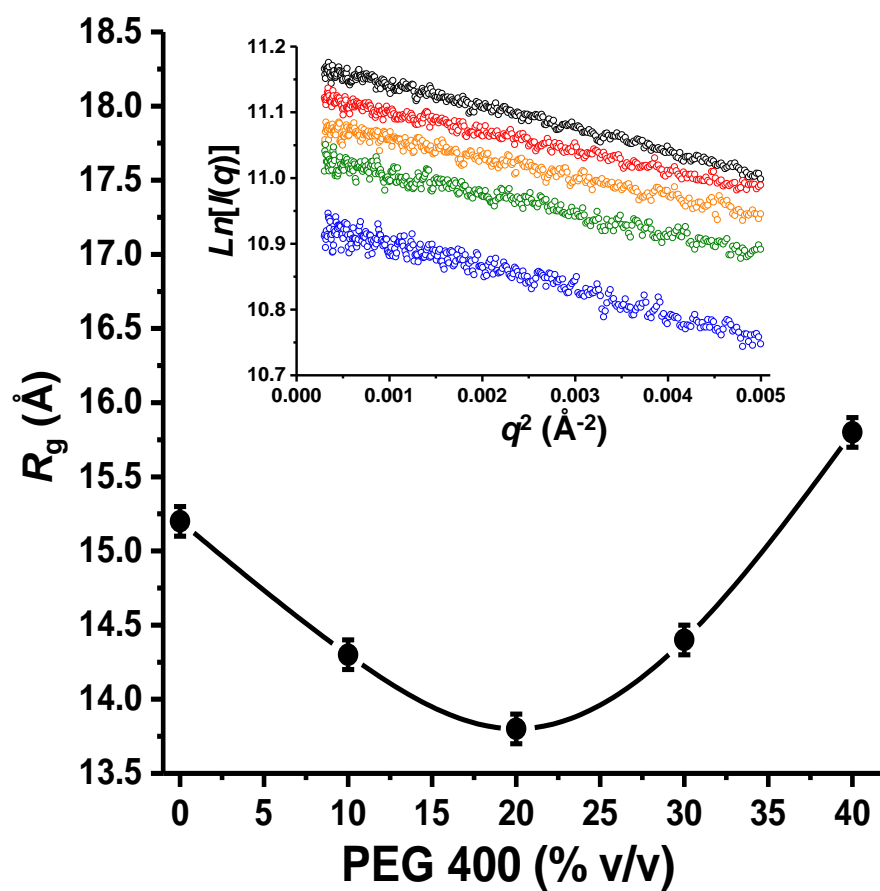


Fig. S7. Effect of PEG 400 on the R_g of PYP. The R_g values with error bars according to the concentration of PEG 400. (Insert) Guinier plots of each sample (Black: PEG 0% v/v, Red: 10% v/v, Orange: 20% v/v, Green: 30% v/v, and Blue: 40% v/v).

Fig. S8.

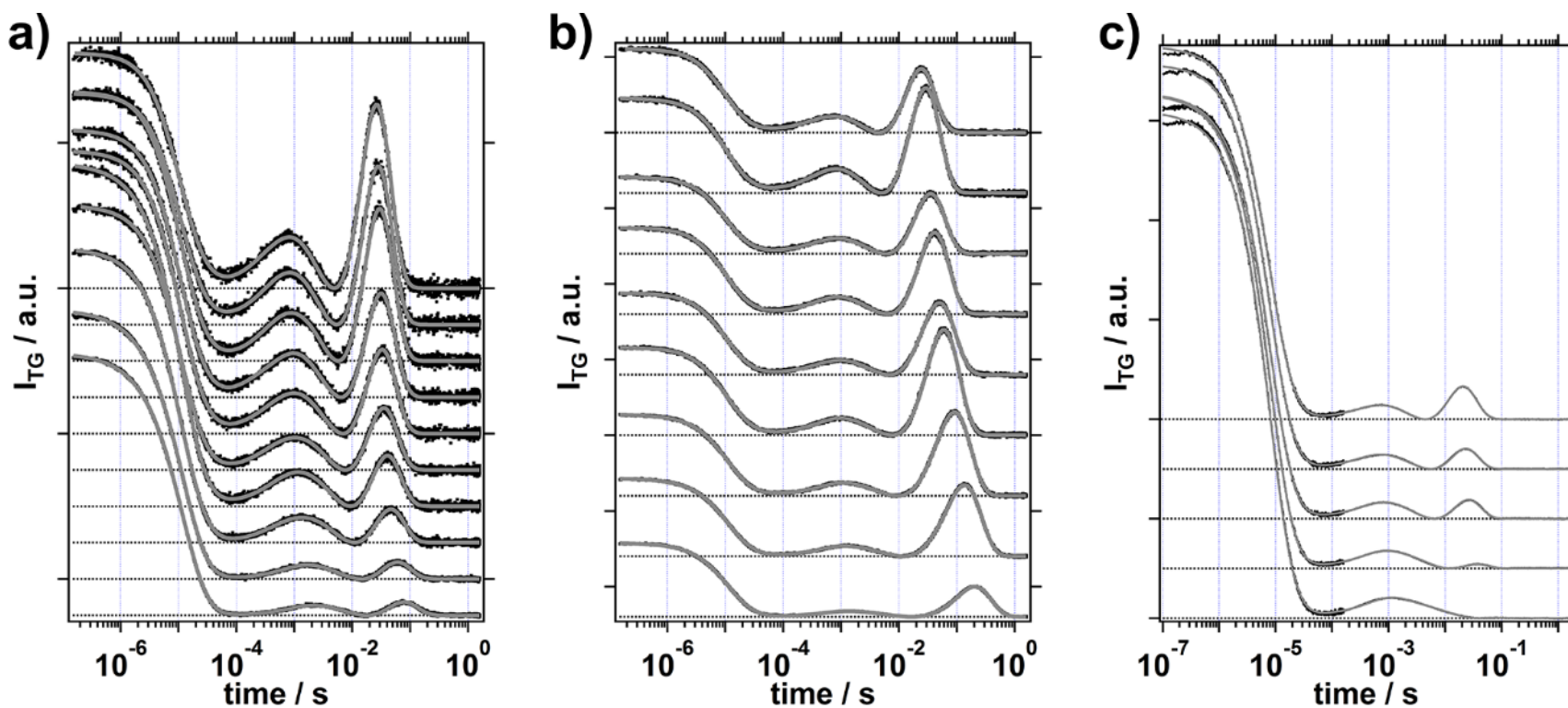


Fig. S8. a) TG signals after photoexcitation of PYP at $q^2 = 3.76 \times 10^{11} \text{ m}^{-2}$ as a function of the concentration of EG. From top to bottom, the concentration of PEG EG are 0, 2, 4, 6, 8, 10, 15, 20, 30 and 40% (v/v). b) TG signals after photoexcitation of PYP at $q^2 = 4.27 \times 10^{11} \text{ m}^{-2}$ as a function of the concentration of PEG 8000. From top to bottom, the concentration of PEG 8000 are 0, 2, 5, 7, 9, 12, 17, 23 and 28% (v/v). c) TG signals after photoexcitation of PYP at $q^2 = 4.4 \times 10^{11} \text{ m}^{-2}$ as a function of the concentration of Dextran 40. From top to bottom, the concentration of Dextran 40 are 0, 2, 4, and 9% (v/v). Experimental signals (black) and theoretical signals (gray) calculated by using Eq. (1) are shown.

Fig. S9.

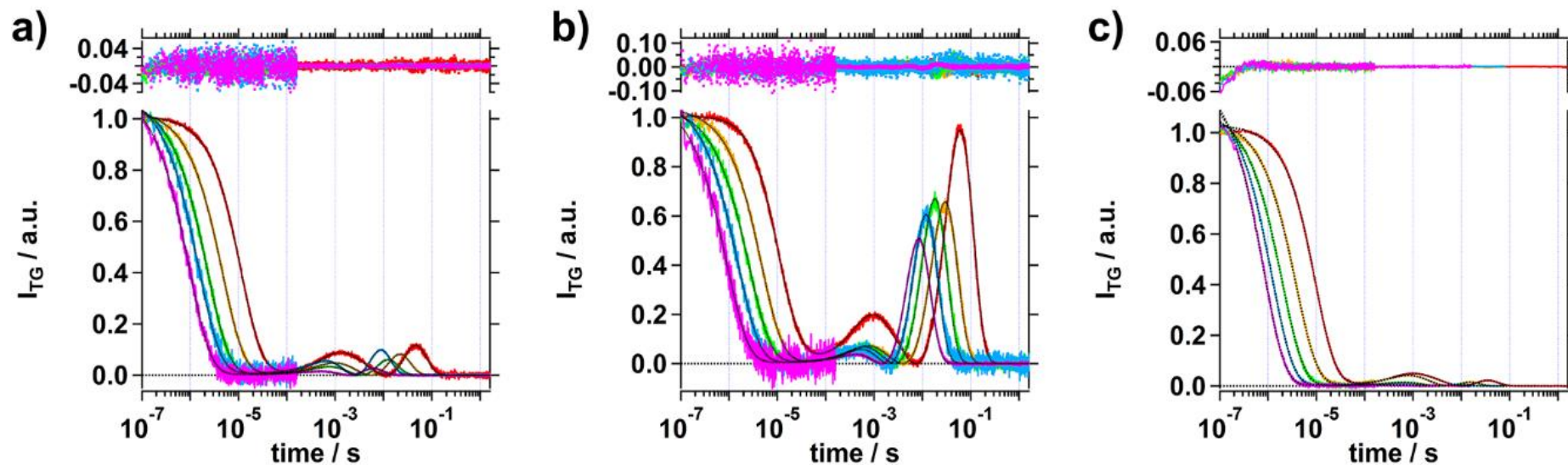


Fig. S9. TG signals of PYP in EG (a), PEG 8000 (b), and Ficoll PM 70 solutions at various q^2 values. a) shows TG signals measured in 20% (v/v) of EG solutions. The q^2 values are 0.40 (red), 0.93 (orange), 1.8 (green), 2.7 (pale blue) and 4.2 (magenta) $\times 10^{12} \text{ m}^{-2}$, respectively. b) shows TG signals measured in 12% (v/v) of PEG 8000 solutions. The q^2 values are 0.43 (red), 0.93 (orange), 1.6 (green), 2.7 (pale blue) and 3.9 (magenta) $\times 10^{12} \text{ m}^{-2}$, respectively. Black dotted lines in all panels are fitting lines by using Eq. (1). c) shows TG signals measured in 6% (v/v) of Ficoll PM 70 solutions, respectively. The q^2 values are 0.44 (red), 1.03 (orange), 1.89 (green), 2.99 (pale blue) and 4.43 (magenta) $\times 10^{12} \text{ m}^{-2}$, respectively.

Fig. S10.

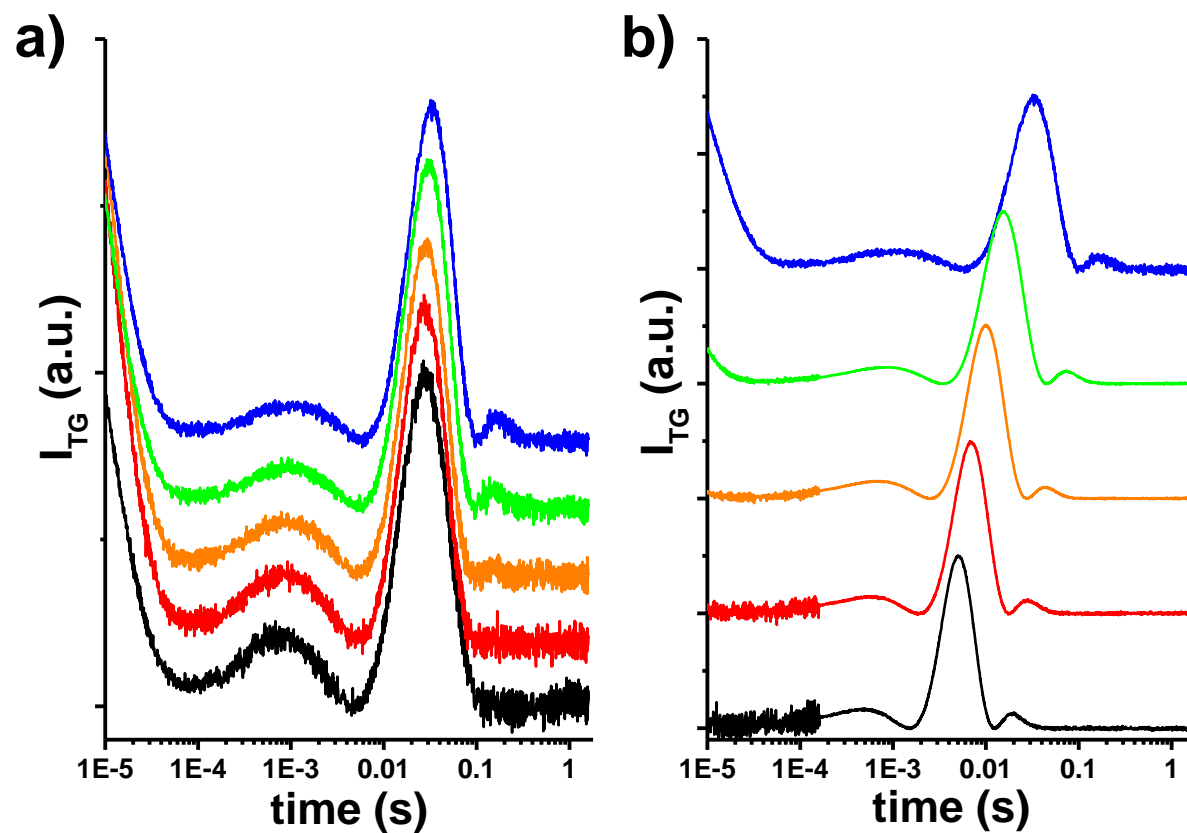


Fig. S10. TG signals. a) TG signals after photoexcitation of PYP at $q^2 = 0.37 \times 10^{12} \text{ m}^{-2}$ as a function of the concentration of BSA. From bottom to top, the concentrations of BSA are 0, 4, 7, 11, and 14% v/v. b) TG signals after photoexcitation of PYP with 200 g/L BSA at various q^2 ranges (From bottom to top, $q^2 = 3.85, 2.62, 1.61, 0.93,$ and $0.37 \times 10^{12} \text{ m}^{-2}$)

Fig. S11.

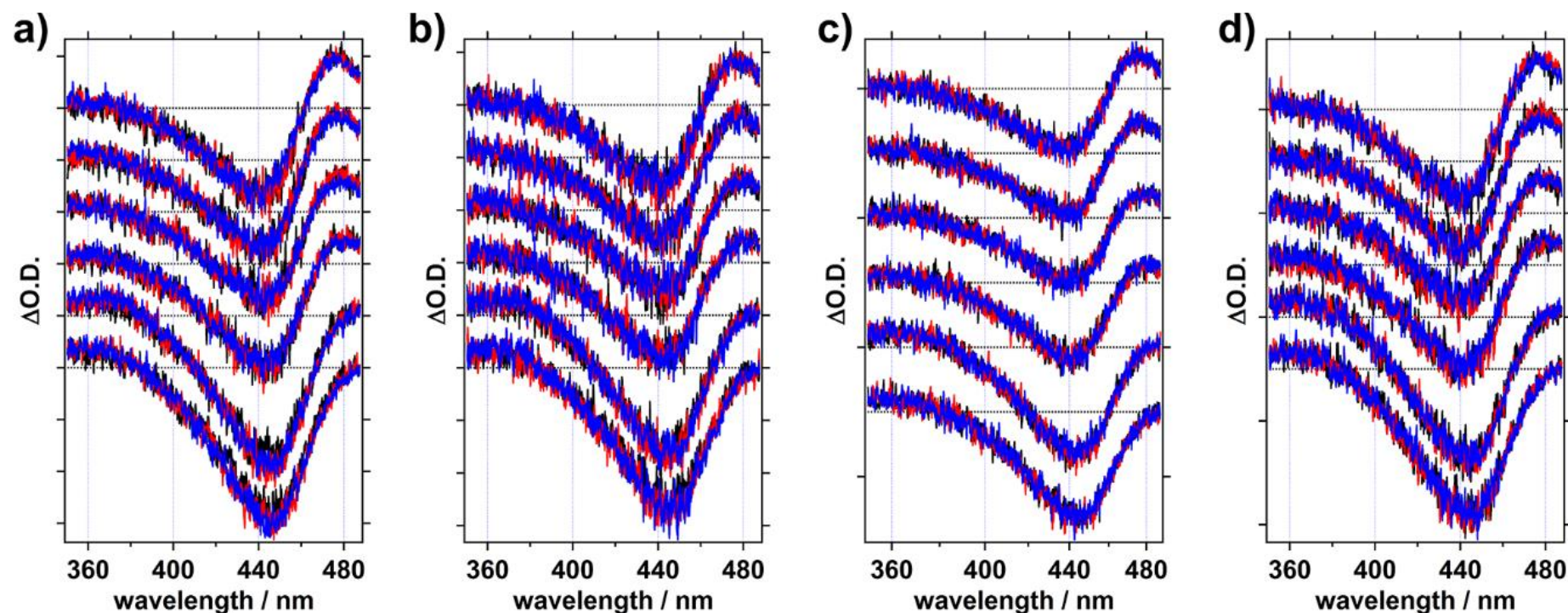


Fig. S11. TA Spectra of PYP in the presence of PEG 1000 (a), PEG 8000 (b), Dextran 40 (c), and BSA (d). a) TA spectra of PYP in 0 (black), 7 (red) and 12% (v/v) (blue) PEG 1000 solutions. b) TA spectra of PYP in 5 (black), 12 (red) and 23% (v/v) (blue) PEG 8000 solutions. c) TA spectra of PYP in 0 (black), 4 (red) and 9% (v/v) (blue) Dextran 40 solutions. d) TA spectra of PYP in 0 (black), 7 (red) and 14% (v/v) (blue) BSA solutions. All TA spectra of PYP in the presence of molecular crowding agents at selected time points are shown (From top to bottom: 100 ns, 1 μ s, 10 μ s, 1 ms and 10 ms).

Fig. S12.

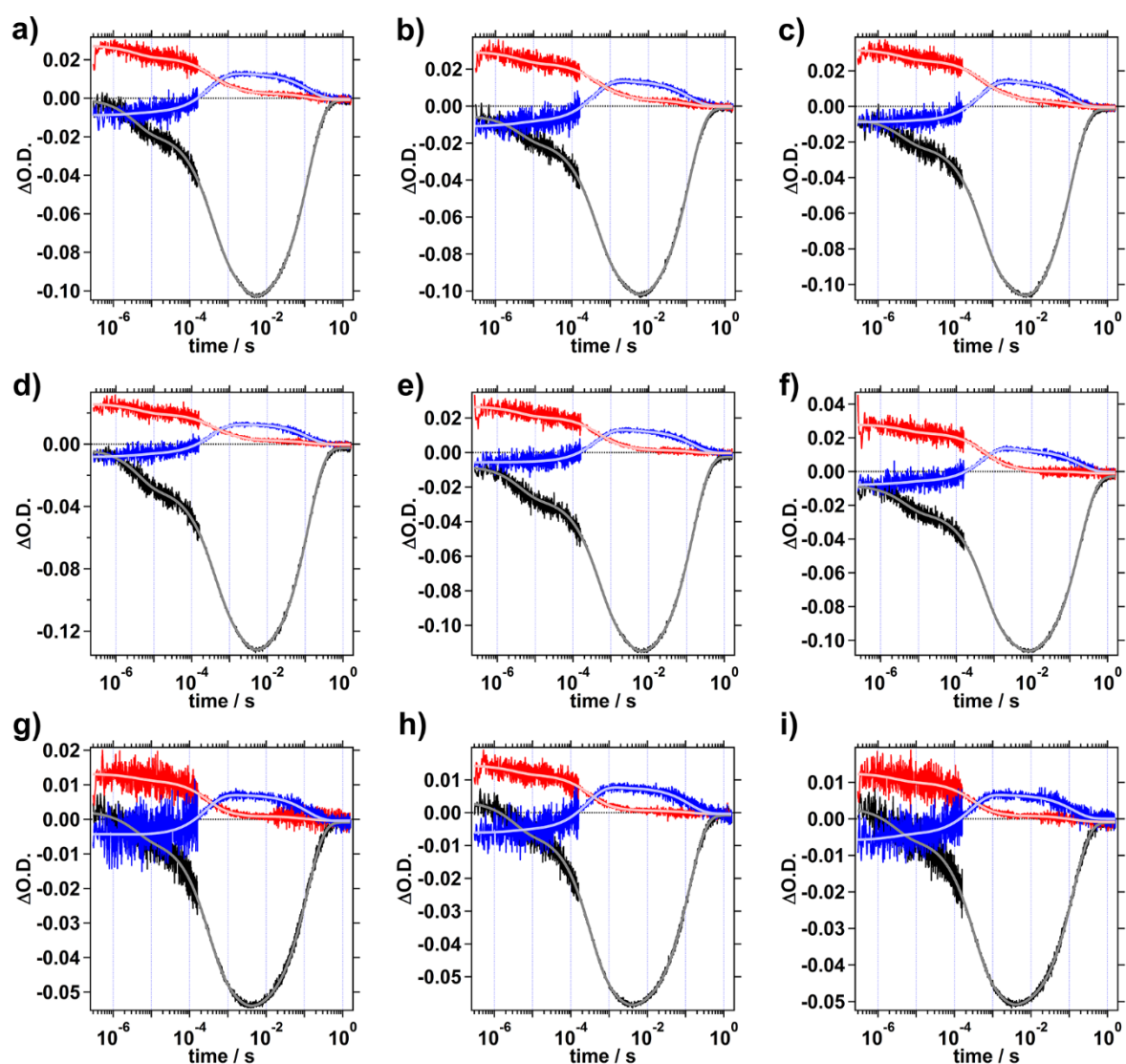


Fig. S12. TA temporal profiles of PYP in EG (a, b and c), PEG 400 (d, e and f), and Ficoll PM 70 solutions. The concentrations of EG are 0 (a), 10 (b) and 20 % (v/v) (c). The concentrations of PEG 400 are 0 (d), 10 (e) and 20% (v/v) (f). The concentrations of Ficoll PM 70 are 0 (g), 4 (h) and 8% (v/v) (i). Three time-dependent signals in each panel were measured at 380 (blue), 465 (black) and 494 nm (red). The fit curves are shown as solid white lines.

Fig. S13.

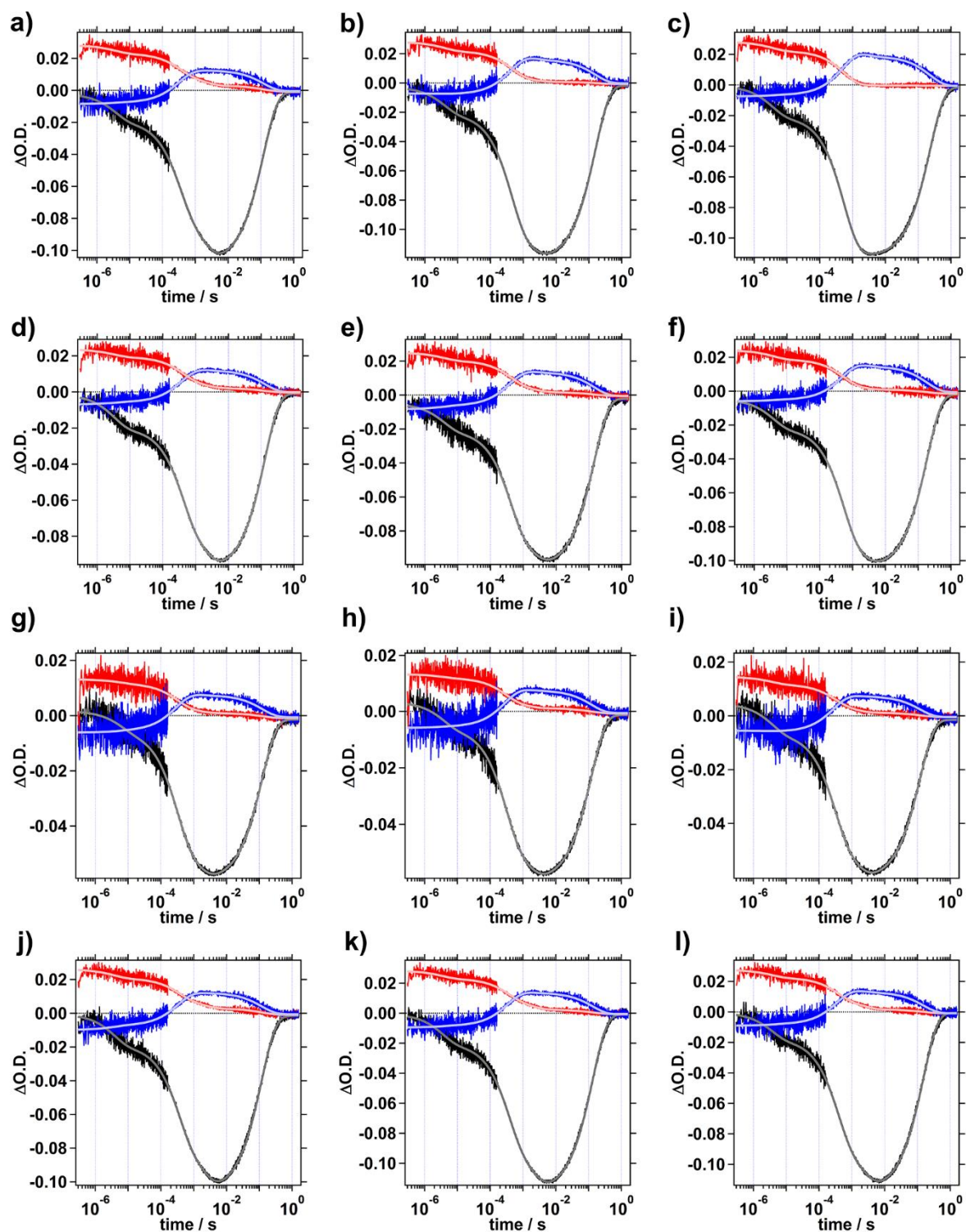


Fig. S13. TA temporal profiles of PYP in PEG 1000 (a, b and c), PEG 8000 (d, e and f), Dextran 40 (g, h, and i), and BSA (j, k, and l) solutions. The concentrations of PEG 1000 are 0 (a), 7 (b) and 12 % (v/v) (c). The concentrations of PEG 8000 are 5 (d), 12 (e) and 23% (v/v)

(f). The concentrations of Dextran 40 are 0 (g), 4 (h) and 9% (v/v) (i). The concentrations of BSA are 0 (j), 7 (k) and 14 % (v/v) (l). Three time-dependent signals in each panel were measured at 380 (blue), 465 (black) and 494 nm (red). The fit curves are shown as solid white lines.

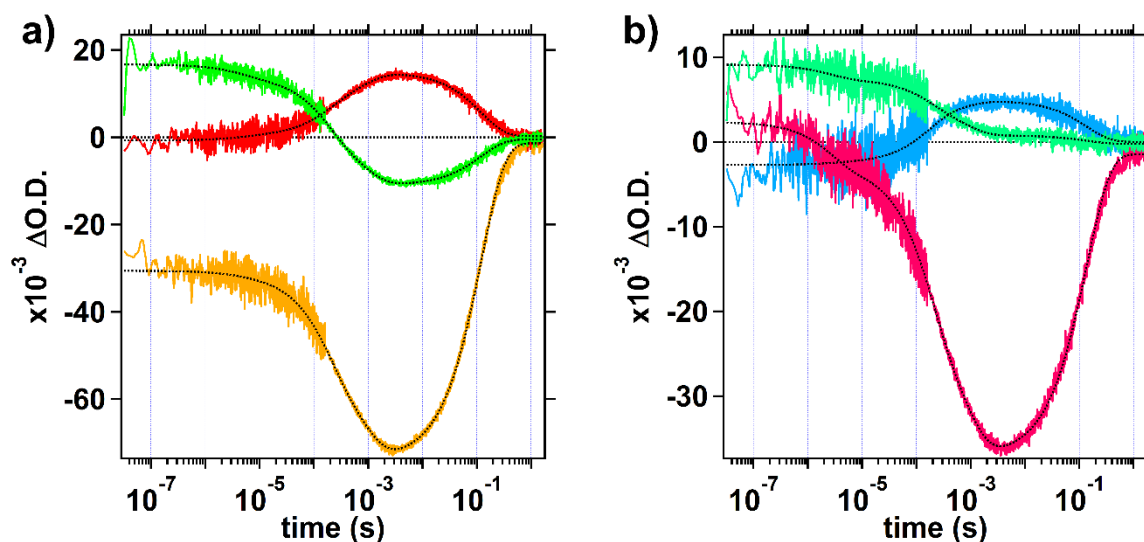


Fig. S14. Transient absorption temporal profiles of wild-type PYP. (a) Three time-dependent signals were measured at 362 (red), 446 (orange) and 477 nm (green). The signals were well-fitted simultaneously by using four exponential functions with offset. Determined time constants by fitting are $4.9 \pm 1.8 \mu\text{s}$, $170 \pm 9 \mu\text{s}$, $810 \pm 30 \mu\text{s}$, and $120 \pm 1 \text{ms}$. (b) Three time-dependent signals were measured at 380 (pale blue), 465 (magenta) and 494 nm (pale green). The signals were well-fitted simultaneously by using four exponential functions with offset. Determined time constants by fitting are $2.6 \pm 0.7 \mu\text{s}$, $160 \pm 12 \mu\text{s}$, $810 \pm 50 \mu\text{s}$, and $140 \pm 1 \text{ms}$. The fit curves are shown as black dotted lines.

References

1. Zhou, H. X.; Rivas, G.; Minton, A. P., Macromolecular Crowding and Confinement: Biochemical, Biophysical, and Potential Physiological Consequences. *Annu. Rev. Biophys.* **2008**, *37*, 375-97.
2. Laurent, T. C., The Interaction between Polysaccharides and Other Macromolecules. 5. The Solubility of Proteins in the Presence of Dextran. *Biochem. J.* **1963**, *89*, 253-7.
3. Rivas, G.; Fernandez, J. A.; Minton, A. P., Direct Observation of the Enhancement of Noncooperative Protein Self-Assembly by Macromolecular Crowding: Indefinite Linear Self-Association of Bacterial Cell Division Protein FtsZ. *Proc. Natl. Acad. Sci. U.S.A* **2001**, *98* (6), 3150-5.
4. Sasahara, K.; McPhie, P.; Minton, A. P., Effect of Dextran on Protein Stability and Conformation Attributed to Macromolecular Crowding. *J. Mol. Biol.* **2003**, *326* (4), 1227-37.
5. Winzor, D. J.; Wills, P. R., Molecular Crowding Effects of Linear Polymers in Protein Solutions. *Biophys. Chem.* **2006**, *119* (2), 186-95.
6. Rubinstenn, G.; Vuister, G. W.; Mulder, F. A.; Dux, P. E.; Boelens, R.; Hellingwerf, K. J.; Kaptein, R., Structural and Dynamic Changes of Photoactive Yellow Protein during Its Photocycle in Solution. *Nat. Struct. Biol.* **1998**, *5* (7), 568-70.
7. Dux, P.; Rubinstenn, G.; Vuister, G. W.; Boelens, R.; Mulder, F. A.; Hard, K.; Hoff, W. D.; Kroon, A. R.; Crielaard, W.; Hellingwerf, K. J., et al., Solution Structure and Backbone Dynamics of the Photoactive Yellow Protein. *Biochemistry* **1998**, *37* (37), 12689-99.
8. Unfortunately, we could not measure the scattering of PYP in the presence of Ficoll PM 70, Dextran, or BSA, because of the intensive scattering signals of the used crowder.
9. Imamoto, Y.; Kamikubo, H.; Harigai, M.; Shimizu, N.; Kataoka, M., Light-Induced Global Conformational Change of Photoactive Yellow Protein in Solution. *Biochemistry* **2002**, *41* (46), 13595-601.
10. Akabayov, B.; Akabayov, S. R.; Lee, S. J.; Wagner, G.; Richardson, C. C., Impact of Macromolecular Crowding on DNA Replication. *Nat. Commun.* **2013**, *4*, 1615.
11. Arakawa, T.; Timasheff, S. N., Mechanism of Poly(ethylene glycol) Interaction with Proteins. *Biochemistry* **1985**, *24* (24), 6756-62.
12. Hammes, G. G.; Schimmel, P. R., An Investigation of Water-Urea and Water-Urea-Polyethylene Glycol Interactions. *J. Am. Chem. Soc.* **1967**, *89* (2), 442-446.
13. Ingham, K. C., Polyethylene Glycol in Aqueous Solution: Solvent Perturbation and Gel Filtration Studies. *Arch. Biochem. Biophys.* **1977**, *184* (1), 59-68.